Composite Cold-Formed Steel Rubberised Concrete Building Framed Systems

Dieudonne Iraguha[1], Derya Deniz[2], Alireza Bagheri Sabbagh[3], Shahabeddin Torabian[4], Naeimeh Jafarifar[5]

[1] Department of Civil Engineering, Özyeğin University, Istanbul, Turkey, dieudonne.iraguha@ozu.edu.tr
[2] Department of Civil Engineering, Özyeğin University, Istanbul, Turkey, derya.deniz@ozyegin.edu.tr
[3] School of Engineering, University of Aberdeen, Scotland, UK, alireza.bsabbagh@abdn.ac.uk
[4] Department of Civil and Systems Engineering, Johns Hopkins University, Baltimore, MD, USA, storabian@sgh.com
[5] School of Architecture and Built Environment, Robert Gordon University, Aberdeen, Scotland, UK, n.jafarifar@rgu.ac.uk

Abstract - In this research, with the use of cold-formed steel (CFS) sections in-filled with rubberized concrete (RuC), a new low-carbon construction system is developed and assessed for its structural resilience and environmental impact compared to the current conventional earthquake-proof construction. First, connection level moment-rotation responses of the new form of CFS-RuC framed structure are validated against the results obtained from detailed finite element analyses. Next, nonlinear pushover analyses are undertaken on the CFS-RuC framed system in conjunction with conventional hot-rolled steel and reinforced-concrete (RC) frames for a case study selected in Istanbul. Lastly, economic and environmental impact analyses are conducted on the frame systems. The results show that the new CFS-RuC composite system offers both structural and environmental advantages compared to conventional systems. In terms of seismic performance of multi-storey buildings, it is shown that the ductility capacity of the CFS-RuC system can be improved by increasing the number of stories.

Keywords: Rubberized concrete, Cold-formed Steel, Carbon footprint, Semi-rigid connections, Seismic performance.

1. Introduction

Given both the high seismicity of Turkey's most populated city, Istanbul and its prominent role in commercial and cultural activities, an urgent need has arisen to seek sustainable mitigation plans to reduce the devastating effects of probable future earthquakes in this city. Most importantly, in the face of global climate emergencies, plans to be adopted should ensure that drastic reductions in carbon emissions are a priority. Therefore, while preparing for disasters, many efforts should be invested in addressing carbon emissions associated with the construction process.

Presently, the industrial sectors responsible for 25% of the global CO_2 focus on minimizing the use of virgin materials by increasing the use of recycled materials, which are destined to be stockpiled if not recycled. Recently, the potential of using rubber from scrap tires in the construction sector has been studied [1]. Studies show that adding rubber to normal concrete results in more energy-dissipative concrete with increased ductility [2], which is desirable in high seismic zones like Istanbul. In addition to their high performance, concrete composites which utilize recycled tires as aggregates have the potential to reduce overall greenhouse gas emissions, provide potential economic benefit and reduce the environmental issues associated with end-of-life tires as compared to conventional concrete [1]. Moreover, seismic shaking table tests demonstrate that adding rubber crumbs can reduce the seismic force on concrete structures due to the increased damping, therefore permitting designs with fewer materials. At the same time, concerns about the reduction in compressive strength of rubberized concrete have been raised, which is attributed to the poor bonding between the rubber particles and the cement paste [2].

To solve this poor bonding problem, a new composite system comprising rubberized concrete (i.e., concrete with rubber aggregates; RuC) infilled into cold-formed steel tubes (CFS) has been recently proposed [3]. Fig. 1 shows a detailing of the developed composite CFS-RuC semi-rigid moment-resisting (MR) connection. The connection comprises a CFS tubular beam connected to both sides of a CFS tubular column through side plates and infilled with RuC [3]. The new composite system uses some features of Lightweight Steel Framing system (LSF), a prevalent framing system among many researchers and engineers. Within this LSF system, one of the major concerns is that they are designed with a considerable number of

underutilized sections [4]. To address this issue, the role played by connection configurations is critical in facilitating full strength usage of LSF sections and improving the ductility capacity. Therefore, an earlier study by the authors has focused on detailed finite element (FE) analyses of various connection configurations of the rubberized concrete-filled steel tube sections (CFS-RuC) [3]. Using these FE results [3], this paper extends the work and explores its applicability to the frame level analysis by conducting a validation study.
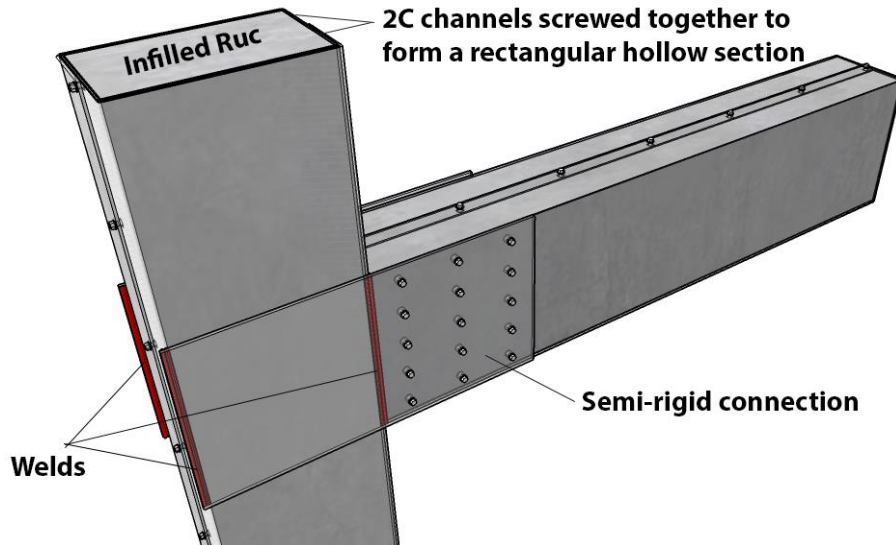

Fig.1: Details of the rubberized concrete-filled steel tube system (adopted from [3])

This paper first develops a practical plastic hinge model (i.e., moment versus rotation) representing the performance of the new frame system's connection (Fig.1) through a validation study. Then, frame-level performance analyses are conducted on different frame structures using the developed connection model and results from the validation study. Eventually, an economic/environmental impact assessment is implemented to evaluate the low carbon sustainability of the new composite system. Among anticipated advantages of this new system, when compared to conventional steel or reinforced concrete systems, include the following: the restraining effect of rubberized concrete makes the local buckling of the steel tube postponed and mitigates the strength deterioration after local buckling, therefore enhancing energy dissipation capacity in the post-yield response. In addition, the environmental burden can be reduced by omitting formwork and bypassing the extraction of virgin aggregates; hence CO_2 emitting actions involved in acquiring those aggregates are avoided. Moreover, potential fire threats and pollution caused by stockpiles of rubber shreds can be avoided by storing these materials as aggregates inside the RuC members.

2. Plastic Hinge Model for CFS-RuC Connections

The finite element (FE) results obtained in the earlier study [3] provide a basis for justifying the practicality of the infill RuC in eliminating unwanted limit states and improving the moment-rotation response. However, finite element analyses [3] require too much computation effort and hence are not practical to perform frame-level analyses. A plastic hinge model is therefore developed through a validation study with the corresponding FE results to come up with an applicable modeling protocol that can be used in the frame-level analysis.

In this study, connection configurations are labeled with abbreviations that start with CFS-RuC, then the beam and column thicknesses (2, 3, or 4 mm) respectively, followed by side plate thicknesses (SP4, 6, or 8 mm) and the number of screw connection arrays (#15, 24, 36 or 42) ended by corresponding gravity loading (60, 300, 600 kN) considered in the connection design. For example, CFSRuC2-4-SP4#24-300 stands for a CFS-RuC connection with a CFS beam thickness of 2 mm and a CFS column thickness of 4mm, using a side plate thickness of 4mm with 24 screws and 300 kN of gravity loading applied at top of the column. Totally fifteen different connection configurations are considered in the study.

A shell type FE model using Abaqus [6] developed in the earlier study [3] and a corresponding beam type model using SAP2000 [5] developed in this study are shown in Fig. 2a and Fig. 2b, respectively. The models represent a one-way

cantilever connection component delineated between the inflection points of a 4 m span moment-frame under unity displacement-controlled loading. In the SAP2000 model (Fig. 2b), the beam and column composite sections are modeled in the section designer by assuming the unconfined concrete model for the RuC infill. Frame elements are used to model the beams and columns. A hinge model composed of a plastic and an elastic spring element incorporating total moment(M)-rotation(θ) response for the connection is modeled at the beam-column ends using M- θ curve data extracted from the accompanying connection FE results [3]. Both the hinge and elastic spring are assigned with an offset at the end of the connection element, which provides a close estimate of the pushover results as the one from the shell type model for Abaqus [3]. The boundary conditions and gravity loading specifications are set to be the same as of the shell type model [3].
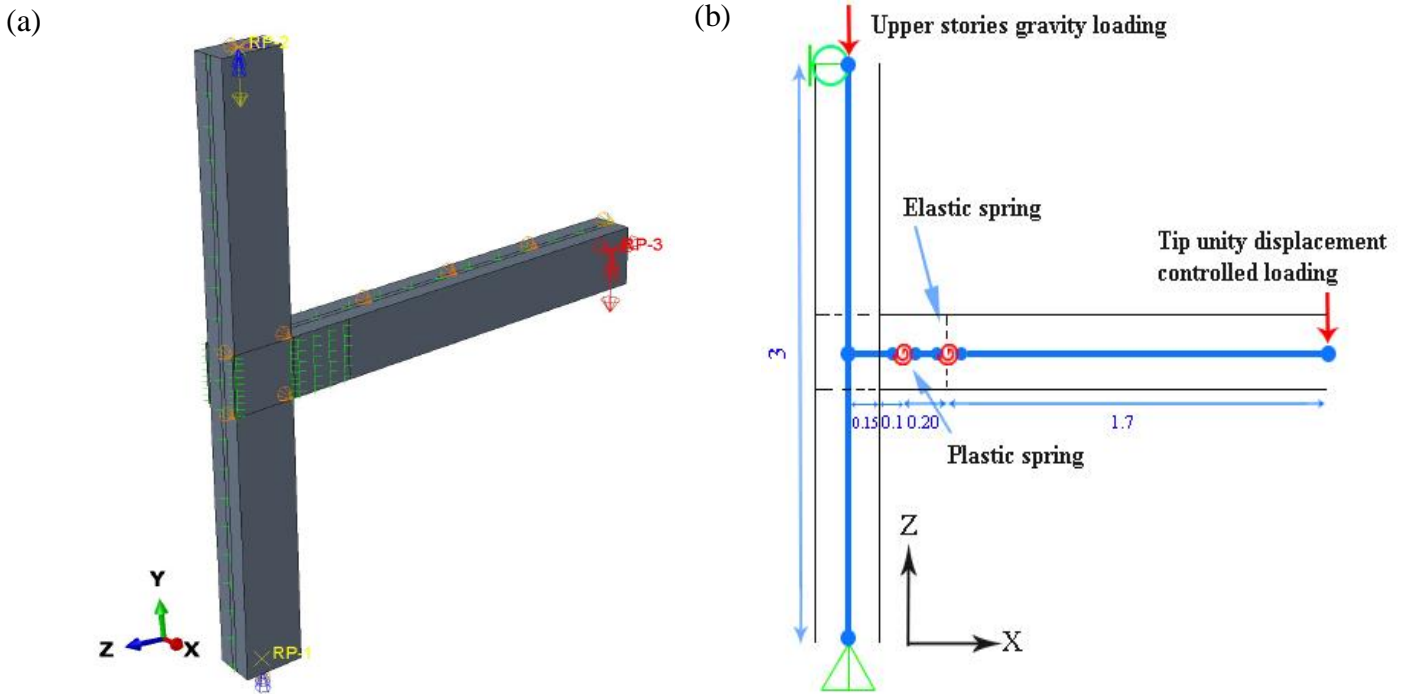

Fig. 2: Modeling details of a composite CFS-RuC connection: (a) shell model in Abaqus [3] and (b) beam model in SAP2000 (units in m)

For a composite CFS-RuC connection (CFSRuC2-4-SP4#24-300), Fig. 3a illustrates the moment-rotation (M-θ) curve (dashed line) obtained from the Abaqus results. The linear line (solid line) represents the slope of the elastic portion of the M-θ curve, from which the stiffness of the elastic spring element is deduced and assigned at the beam-end in the SAP2000 model. Further, the remaining portion of the curve (solid line with a star marker) represents plastic rotation data interpolated from M-θ curve to be assigned as a 'plastic' hinge at the beam-end in the SAP2000 model. These properties are very essential for proper definition of the new CFS-RuC system's semi-rigid connection. The hinge overwrite property is assigned in the SAP2000 program to ensure accurate results.

For the same connection, Fig. 3b displays pushover curve results from SAP2000 compared with the corresponding force-displacement curve from Abaqus results. Matching pushover results as displayed in Fig. 3b are achieved through modifying program parameters such as plastic and elastic spring locations and recording how each property affects the results. Eventually, all optimum modeling properties that ensure close results when compared to Abaqus results are obtained as reported in Table 1 (in terms of elastic stiffness, spring's location from the beam-column joint, and five points A, B, C, D, and E to define moment-rotation behaviour), thus concluding the validation study for the development of a hinge-model.
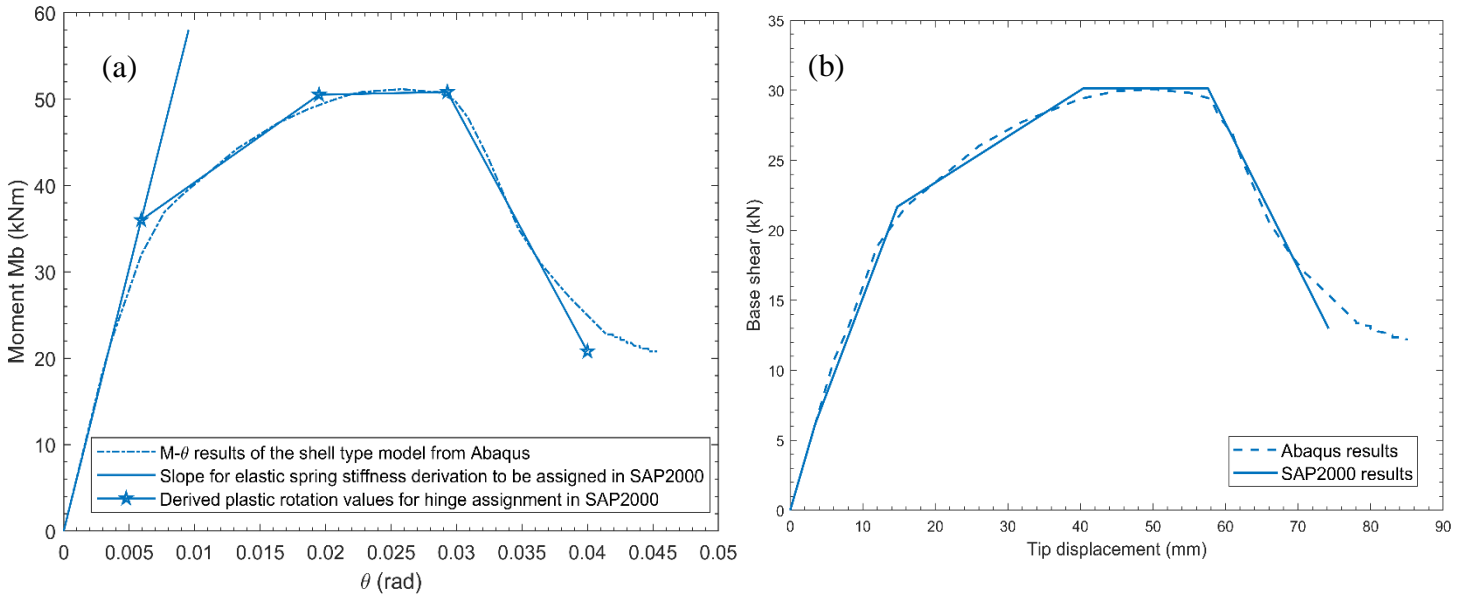
Fig. 3: For the representative connection configuration CFSRuC2-4-SP4#24-300: (a) elastic spring and moment-rotation curves used in the hinge model and (b) pushover results

Table 1: Plastic hinge and elastic spring assignments to beam-column joints (Mn is the yield moment of the bare steel section, which is 33 kNm and 64 kNm for the CFSRuC2 and CFSRuC3 connection configurations, respectively)

Label	Elastic spring stiffness (KNm/rad)	Plastic hinge location (m)	Elastic spring location (m)	Parameters									
				A		B		C		D		E	
				M/Mn	Θ	M/Mn	Θ	M/Mn	Θ	M/Mn	Θ	M/Mn	Θ
CFSRuC2-4-SP4#15-60	5643	0.2	0.4	0	0	0.77	0	1.1	0.0073	1.1	0.012	0.64	0.018
CFSRuC2-4-SP4#15-300	5643	0.2	0.4	0	0	0.77	0	1.1	0.0073	1.1	0.012	0.38	0.0217
CFSRuC2-4-SP4#15-600	6250	0.2	0.45	0	0	0.8	0	1.16	0.0089	1.16	0.010	0.79	0.0168
CFSRuC2-4-SP4#24-60	6610	0.25	0.45	0	0	1.16	0	1.67	0.0109	1.67	0.0216	0.82	0.0355
CFSRuC2-4-SP4#24-300	6082	0.4	0.45	0	0	1.09	0	1.54	0.0114	1.54	0.0209	0.63	0.0376
CFSRuC2-4-SP4#24-600	6610	0.25	0.45	0	0	1.24	0	1.7	0.0125	1.67	0.0217	1.03	0.0314
CFSRuC2-4-SP6#24-60	7000	0.25	0.5	0	0	1.23	0	1.7	0.0085	1.45	0.015	0.55	0.0249
CFSRuC2-4-SP6#24-300	7500	0.25	0.5	0	0	1.22	0	1.71	0.0098	1.66	0.0133	1.1	0.0192
CFSRuC2-4-SP6#24-600	6981	0.25	0.45	0	0	0.75	0	1.12	0.0097	1.09	0.0128	0.69	0.0192
CFSRuC3-4-SP4#24-300	7773	0.25	0.4	0	0	1.25	0	1.66	0.013	1.66	0.0203	0.16	0.0363
CFSRuC3-4-SP6#24-300	7885	0.25	0.45	0	0	1.24	0	1.75	0.0083	1.75	0.0107	0.12	0.0315
CFSRuC3-4-SP6#36-300	8714	0.25	0.45	0	0	0.95	0	1.25	0.0118	1.09	0.0184	0.19	0.0323
CFSRuC3-4-SP8#36-300	9000	0.25	0.45	0	0	0.87	0	1.16	0.0067	0.88	0.0181	0.23	0.0311
CFSRuC3-4-SP6#42-300	9000	0.25	0.45	0	0	1	0	1.35	0.0154	1.35	0.0284	1.06	0.0445
CFSRuC3-4-SP8#42-300	9560	0.25	0.45	0	0	1.02	0	1.36	0.0077	1.34	0.0148	0.17	0.032

3. Frame Performance: A Case Study of 3 Story-Frame

Using the modelling parameters proposed for the connection configurations in the validation study above (see Table 1), the frame performance of the new CFS-RuC system can easily be evaluated. However, due to the lower number of sections available for the new system in Table 1, relevant assessments are carried out on those sections to come up with a case study and it is accomplished through examining the maximum number of stories that they can sustain. Here, the governing criteria is that the frame system's section capacities should surpass seismic demands resulting from the equivalent seismic lateral force method. Consequently, this study is limited to a case study of 2D 3-story frame, as indicated by the analysis results. The 3-story two-bay frame structures in consideration consists of a bay width of 4m and a story height of 3m, with no structural irregularities, and is assumed to be situated in the highly seismic region of Bayrampaşa/Istanbul in Turkey.

To compare seismic performance of the proposed composite frame, three different types of frame structures, are also considered: a conventional hot-rolled steel frame, a conventional reinforced concrete frame, and a bare version of the same proposed cold-formed steel (CFS) frame system without any inclusion of infill RuC. However, all frames except the bare CFS frame are designed in accordance with the current Turkish Building Earthquake Code (TEC 2018) [7]. The bare CFS frame is solely included in the comparison to examine how the presence or absence of RuC infill affect the overall CFS-RuC system's behaviour. Table 2 contains the structural member's material properties and dimensions, where only one beam and one column sections are chosen for each of the four frame systems. The CFSRuC2-4-SP4#24-300 connection configuration is assigned to all beam ends of the proposed composite frame system (CFSRuC) as it exhibits high ductile behaviour. Apart from having close yielding flexural capacities for each element, all systems have been evaluated for various safety and deflection requirements based on the TEC 2018 [7].

Table 2: Dimensions and material properties of the structural members considered in the case study

Frame structure	Beams (mm)	Columns (mm)	Material property (N/mm^2)
Composite CFS-RuC (with semi-rigid connections)	CFSRuC2-4-SP4#24 175* x 300, t= 2mm	CFSRuC3-4-SP6#42 175* x 300, t= 3mm	C21, S275
Bare CFS (with semi-rigid connections)	The same with above but no RuC inside	The same with above but no RuC inside	S275
Conventional Steel (with rigid connections)	W200x15	W250x22.3	S275
Conventional RC (with rigid connections)	250x300	300x300	C25, S420

*Note that these sections are built-up from two overlapped C-sections and RuC

3.1. Moment-rotation Comparison

In structural frame modeling, plastic hinges are usually assigned at the end of the column and beam elements since that part undergoes huge plastic deformations under seismic loading. As the development of composite sections is based on the strong column-weak beam theory (SCWB) [3], hinges are assigned to all beam members' ends and only at the base for columns. While moment-rotation values reported in Table 1 are used to assign plastic hinges for the new composite frame members, hinge properties for conventional frame members are derived from ASCE41-13 tables [8]. Fig.4a illustrates the moment-rotation curves of the four systems in comparison. The moment-rotation curve for conventional steel displays the largest rotation values as an indication of high ductility. While all systems have around the same yielding flexural strength, the CFS-RuC frame has the highest ultimate flexural capacity. The major differences and similarities spotted here are expected to be reflected again in the force-displacement curves of the nonlinear static analyses.

3.2. Pushover Analysis Results

The nonlinear static pushover analysis results can be used to evaluate lateral resistant capacities of all four frames and estimate the potential ductility of the structures. SAP2000 program is used to perform pushover analyses. The resulting capacity curves are depicted in Fig.4b. Notice that all curves portray a deterioration part, which indicates failure. This is due

to the assignment of hinge overwrites property being assigned, which meshes the frame element around the hinge and so ensures good results. Moreover, considering the P-delta effects in the analyses might stimulate such behaviour too. From the capacity curves, the yield and maximum base shears of the composite CFS-RuC frame structure are higher than those of the conventional steel, RC, and bare CFS frame structures, implying that CFS-RuC frame is more earthquake-resistant than the other three. Additionally, Fig. 4b shows that the CFS-RuC frame is attaining large displacements before failure when compared to the RC frame.
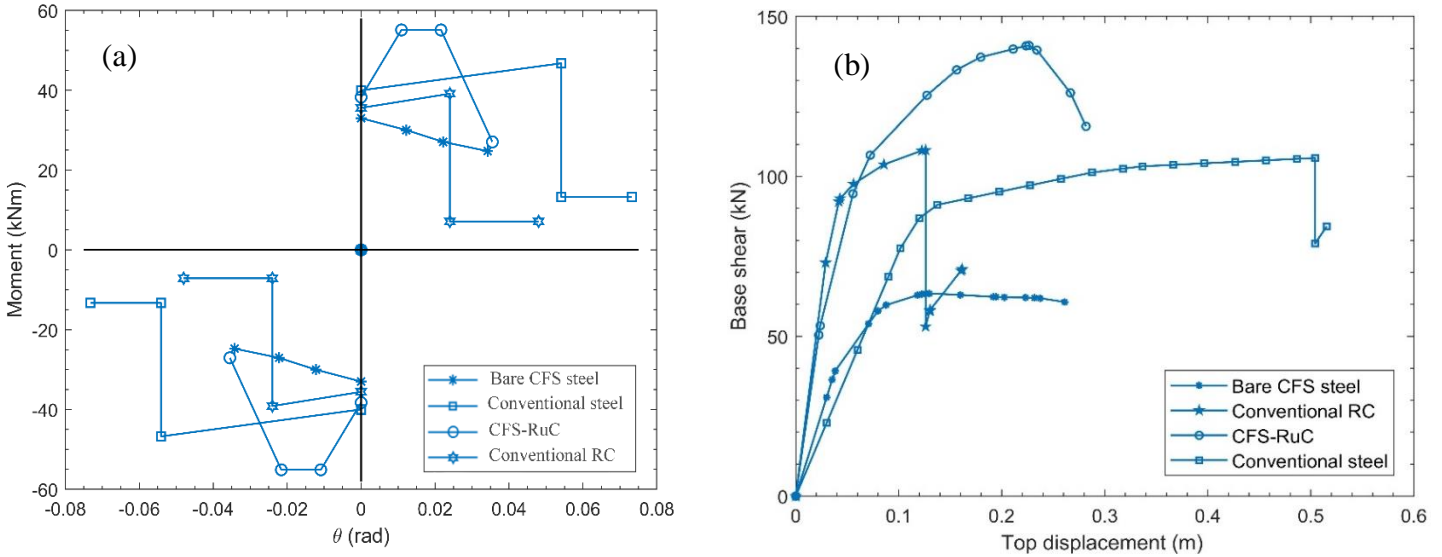

Fig. 4: Comparison of the four types of 3-story frame structures: (a) the hinge models (moment-rotation curves) used in the frame system, and (b) capacity (pushover) curves

In Fig. 4b, the reason behind the slight difference observed in the initial stiffness of capacity curves for the CFS-RuC and RC frames is the fact that the RC frames have rigid connections while CFS-RuC frames have semi-rigid ones. The lowest base shear and soft initial stiffness are observed in the steel frame capacity curve, and this can be attributed to different aspects as one being that steel sections have small areas, thus low strength. However, they are flexible enough to attain large displacements with their high deformation capacity, as observed in the capacity curves. On other hand also, the observed high deformation capacity of the conventional steel frame can be possible because no P-M interaction is accounted for in column base connections in the frame analyses due to the rough assumptions that the gravity loading is relatively low. Otherwise, such steel frames usually buckle early in the study when the interaction is included and thus leading to poor ductile behaviour than what is presented in Fig. 4b.

Comparing the results between the CFS-RuC frame and bare CFS steel frame in Fig. 4b is very crucial to understand the effect of the presence of rubberized concrete infill in the cold-formed steel tubes. As expected, the bare CFS frame's base shear is very low due to the lack of infill RuC that would restrain the outer steel section from local buckling and would allow the system to attain its full base shear capacity. This again shows how well the new composite system is equipped with desirable properties for seismic-resistant building design. This is proven by maintaining a good balance between high base shear capacity (among all systems) and adequate ductility (more elevated than its counterpart RC). It has also been noticed that both bare steel and conventional steel frames have close initial stiffness. This results from both materials sharing the exact material definition (steel) and relative flexural stiffness (EI) value.

Extensive parametric studies are currently being performed on the same frame types to account for the impacts of structural model changes on the performance estimates. As a part of these parametric studies, one attempt has been made exclusively to determine to which extent the ductile behaviours of all frames with increased number of stories would differ when compared to the 3-story (low-rise) structure, considering the same sections and gravity loading conditions. Favourably, it has been observed that the CFS-RuC system shows high potential of demonstrating improved ductile behaviour as number of stories increases.

4. Environmental and Economic Impact Assessment of the CFS-RuC Buildings

Table 3 summarizes the overall material cost values of the conventional and proposed frame structures, as well as their embodied CO_2 amounts resulting from material use, with the purpose of just undertaking a 'preliminary' impact assessment. The unit prices for all material and embodied carbon emissions amounts are collected from the 2021-unit price archive of the Turkish Ministry of Environment and Urbanism [10] and the study by [9],[11], respectively.

Table 3: Material cost and carbon footprint estimations for the 3-storey frame structures

Frame structure	Components	Weight (kN)	Amount used for material price calculation		Unit material price (TL)	Total material price (TL)	Final material price (TL)	Unit Embodied Carbon kg-CO_2/kg	Total Embodied Carbon kg-CO_2	Total EC kg-CO_2
Reinforced concrete	C25 ready concrete	100.77	4.23	m^3	198	838	**3257**	+0.1	+1007	**1704**
	Longitudinal reinf.	4.032	411	kg	4.79	1969		+1.38	+567	
	Transverse reinf.	0.922	94	kg	4.79	450		+1.38	+130	
The new CFS-RuC system	C channels	9.83	1000	kg	5.35	5350	**5863**	+1.38	+1382	**1558**
	Concrete with Virgin Aggregates (60%)	36	1.55	m^3	198	307		+0.1	+367	
	Concrete with Rubber Aggregates (40%)	24	1.04	m^3	198*	206		+0.1 -0.178$^{\#}$ = - 0.078	-191	

*Assumed the same price with the use of virgin aggregates. $^{\#}$For reducing CO_2 by storing rubber inside the sections [12].

Results show that the CFS-RuC frame gives more minor carbon emission amounts than RC frames, and it has been observed that this difference can be more significant as the number of stories increases. While the total material price appears to be less for the RC frame, it should be noted that not all cost aspects are taken into account (e.g., cost for formwork and labor costs for detailing are expensive for RC structure construction). Therefore, the results in Table 3 should be considered with attention, after all they still highlights the high potential of CFS-RuC frame in carbon emission reduction. Further studies should be conducted to perform a complete and more realistic impact assessment, considering the material-related impacts and all other factors (e.g., cost and carbon emission related to transportation of materials).

5. Conclusion and Future Research

A new composite frame system featuring lightweight steel framing and rubberized concrete has been introduced and compared to conventional frame systems in terms of seismic performance and impact assessment. The overall results reveal that the seismic performance of the new system is higher to the RC system in terms of ductility. Moreover, it results in a well-balanced seismic response offering higher base shear and adequate deformation capacity. Additionally, incorporating rubber into the CFS-RuC system provides a low carbon footprint when compared to the RC frame, which is a dominant construction type in Istanbul's building stock. Finally, while the CFS-RuC system's construction material price may be relatively high when compared to RC systems, it offers both structural and environmental benefits that are critical for this study. While this study partly highlights better structural performance and low carbon sustainability of the CFS-RuC frame system, it should be remembered that this is just a preliminary assessment with limitations such as: a low number of sections is used in the design; few embodied carbon factors are considered in carbon footprints calculations; and 2D analysis is performed instead of 3D analysis as prescribed by the code. As a result, future work is needed to perform a well-detailed, more realistic assessment for the CFS-RuC frames addressing these prescribed issues and many other areas that require more refinement.

6. Acknowledgement

7. References

[1] Kashani Al, Ngo T. D, Mendis & Hajimohammadi "A sustainable application of recycled tyre crumbs as an insulator in lightweight cellular concrete." *Journal of cleaner production* 149 (2017): pp.925-935.v

[2] Xue, J., & Shinozuka, M. (2013). Rubberized concrete: A green structural material with enhanced energy-dissipation capability. *Construction and Building Materials*, *42*, pp. 196-204

[3] Sabbagh, A. B., Jafarifar, N., Deniz, D., & Torabian, S. (2022, June). Development of composite cold-formed steel-rubberised concrete semi-rigid moment-resisting connections. In *Structures* (Vol. 40, pp. 866-879). Elsevier

[4] Bagheri Sabbagh, S. Torabian (2021). "Semi-rigid floor-to-wall connections using side-framed lightweight steel structures: Concept development", Thin-Walled Structures, 160,107345

[5] SAP2000 Integrated Software for Structural Analysis and Design," Computers and Structures Inc., Berkeley, California

[6] Abaqus Analysis User's Manual, (2019). version 6.21.

[7] TBEC 2018, Turkish Building Earthquake Code, Disaster and Emergency Management Ministry, Ankara (2018)

[8] ASCE 41-13: Seismic evaluation and retrofit rehabilitation of existing buildings. (2012)

[9] Urian, Gabriel Mircea, and Alina Haupt-Karp. "Reduced Carbon Footprint with Composite Structures." *Procedia Technology* 22 (2016): pp.282-289.

[10] Unit price archive yuksek fen kurulu baskanligi (2021)

[11] M.B. Ali, R. Saidur, M.S. Hossain, A review on emission analysis in cement industries, Renewable Sustainable Energy Rev. 15 (5) (2011) pp.2252–2261.

[12] Van Gijlswijk, R. N., Pascale, S., De Vos, S. E., Urbano, G., & alla Dogana, V. I. S. N. (2015). Carbon footprint of concrete based on secondary materials. *Heron*, *60*(1/2), 113.